

Simulation of Fick's Verification of the 2nd Law

Richard DiDomizio*, Afina Lupulescu[†], Martin E. Glicksman[†]

*General Electric Global Research, Niskayuna, NY, 12309, USA.

[†]Materials Science and Engineering Department
Rensselaer Polytechnic Institute
Troy, New York, 12180-3590, USA

Corresponding author: Richard DiDomizio, General Electric Global Research,
Niskayuna, NY 12309, E-mail: didomizrerd.ge.com

December 6, 2005

Key words: Fick's second law, funnel experiments, random walk

Abstract

Adolph Fick's original diffusion experiments used two vessels containing water and salt to establish a steady-state concentration gradient that demonstrated the validity of what is now called Fick's second law of diffusion. The first vessel had a cylindrical shape creating a linear gradient. The second vessel was shaped like a funnel having a correspondent variable flow area. Using Fick's second law, general solutions for any shape of the vessel are developed for steady diffusion in two and three dimensions, respectively. Two dimensional random walks were performed via computer simulations, and the numerical results are compared to continuum theory. Provided that a sufficiently large number of steps are simulated to allow the random walkers to traverse the total diffusion path, good agreement is achieved between discrete "molecular" motions (random walk) and the classical continuum description provided by scalar field theory (partial differential equations).

1 Introduction

The initial verification of Adolph Fick's second law was provided by his now famous salt diffusion experiments [2]-[8], [15]-[19]. Fick placed a layer of sodium chloride (NaCl) crystals at the bottom of two differently shaped vessels connected to large reservoirs of fresh water. Although his experiments were never described in complete detail, or the scheme explicitly sketched out, the authors assume that they resemble the vessels shown in Figure 1. As the experiment progressed and salt molecules diffused up and out of the vessel, replaced by water molecules, the connected reservoirs at one end of the diffusion vessels were refreshed steadily with pure water to establish eventually a steady-state concentration gradient [2]-[8], [15]-[19]. Fick's measurements [2]-[8] of the NaCl concentration profile, conducted via densitometry, showed that a right-circular cylindrical funnel yields at steady-state a linear variation of density versus distance down the funnel. See Figure 1 left. The conical funnel resembling the one shown in Figure 1, right, yielded instead a non-linear (concave downward) plot of density versus distance. These experimental results matched Fick's theoretical calculations, supporting the validity of his now famous second law of diffusion. Moreover, it was through quantitative comparison of these experiments with theory that Fick introduced the indispensable concept of the interdiffusion coefficient.

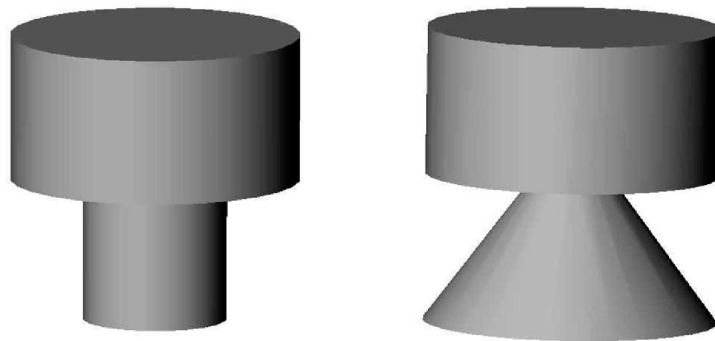


Figure 1: **Left:** *Fick's cylindrical vessel. The wide cylinder above the cylindrical diffusion vessel represents the fresh water reservoir. Right:* *Fick's funnel-shaped vessel. The wide cylinder above the conical diffusion vessel represents the fresh water reservoir.*

2 Solutions to Fick's second Law

2.1 Theoretical Approach

Analytical solutions for the concentration field may be developed easily for steady-state diffusion in two or three dimensions. The derivation of these formulae begins with the linear 2nd-order differential equation for the conservation law now known as the Fick-Jacobs equation [1], which accounts for a variable cross-sectional area for diffusion [2]-[14].

In both two spatial dimensions, \mathbb{R}^2 , and in three spatial dimensions, \mathbb{R}^3 , the Fick-Jacobs equation may be expressed in the linear partial differential form

$$D \left[\frac{\partial^2 C}{\partial x^2} + \frac{\partial C}{\partial x} \frac{1}{A(x)} \frac{dA}{dx} \right] = \frac{\partial C}{\partial t}. \quad (1)$$

In Eq.(1), $C(x, t)$ is the concentration of the salt at location x and time t , $A(x)$ is the locally varying cross-sectional area through which diffusion occurs, and D is the interdiffusion coefficient for salt and water at the temperature and pressure at which the experiment is carried out. As time approaches infinity, the change in concentration with time vanishes, $\partial C/\partial t \rightarrow 0$, and Eq. (1) simplifies to the linear ordinary differential equation

$$\left[\frac{d^2 C}{dx^2} + \frac{dC}{dx} \frac{1}{A(x)} \frac{dA}{dx} \right] = 0, \quad \text{in both } \mathbb{R}^2 \text{ and } \mathbb{R}^3. \quad (2)$$

As indicated, Eq. (2) remains valid for vessels requiring two and three dimensions to describe their diffusion flow geometry.

We create a dimensional frame of reference convenient both for the remainder of the derivation and for the two-dimensional simulations to be discussed. As shown in Figure 2, a cross section of Fick's funnel-shaped vessel is chosen with a running variable, x . The "two dimensional" vessel has a constant thickness, h , into and out of the page, and a variable half-width, $w(x)$, that increases linearly from its minimum value of w_0 at $x = 0$, denoting the upper diffusion boundary with pure water, to a maximum value of w_{max} , at

$x = x_{max}$, denoting the location of the diffusion boundary with the layer of salt crystals. In the case of a cylindrical-shaped vessel, the half-width, w , remains constant over the length of the vessel, from the layer of salt crystals to the fresh water port. For the “three dimensional” conical vessel, $w(x)$ instead is taken equal to the radius, R , of the changing circular cross-section for diffusion, and the symbol h is no longer needed.

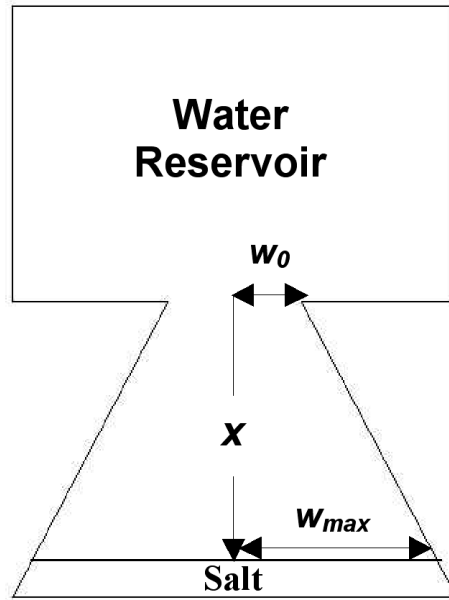


Figure 2: Frame of reference for theoretical calculations and random walk simulations.

Analytical solutions valid in \mathbb{R}^2 and \mathbb{R}^3 are now sought for the steady-state concentration fields, $C(x)$ and $C(R)$, of salt in water throughout the variable section of the diffusion vessels ($0 \leq x \leq x_{max}$). The variation of the area within the vessel in which diffusion occurs needs to be taken into account explicitly, in order to solve for these concentration fields.

In two dimensions the area is $A = w(x) \times h$. In three dimensions the area is $A = \pi R^2 = \pi w^2(x)$. Thus, when these area functions are differentiated and substituted into Eq. (2), the differential equation corresponding to diffusion in the “two dimensional” vessel contains the coefficient -1 , whereas the three-dimensional case contains the coefficient -2 . This difference in coefficients is seen in Eq. (3) for \mathbb{R}^2 and Eq. (4) for \mathbb{R}^3 , following the conversion of the equations to first-order differential equations in which $V = \partial C / \partial x$. The

variable m is the slope of the outer vessel wall. In \mathbb{R}^2 one obtains

$$\frac{dV}{V} = \frac{-m}{w_0 + mx} dx, \quad (3)$$

whereas in \mathbb{R}^3 one obtains

$$\frac{dV}{V} = \frac{-2m}{w_0 + mx} dx. \quad (4)$$

Integrating Eq. (3) and (4) twice leads to Eq. (5) for \mathbb{R}^2 and Eq. (6) for \mathbb{R}^3 . The parameters α_i and γ_i ($i = 2, 3$) are the constants of integration in \mathbb{R}^2 and \mathbb{R}^3 , respectively. Thus, in \mathbb{R}^2 , the concentration field is

$$C(x) = \frac{\alpha_2}{m} \log(w_0 + mx) + \gamma_2, \quad (5)$$

whereas in \mathbb{R}^3 , the concentration field is

$$C(R) = -\frac{\alpha_3}{m} (w_0 + mx)^{-1} + \gamma_3. \quad (6)$$

2.2 Boundary Conditions

The boundary conditions for the steady-state diffusion fields, which are identical in both cases, can now be specified. After a sufficiently long time, the layer of salt crystals at the base of the vessels will fix the concentration of the solution at its equilibrium solubility, C_{max} , when equilibrated at some fixed temperature and pressure. The following constant concentration boundary condition is thereby imposed on the system. In both \mathbb{R}^2 and \mathbb{R}^3 , the saturated layer of salt crystals insures that

$$C(x_{max}) = C_{max}, \quad (x = x_{max}). \quad (7)$$

The presence of a large water reservoir of pure water connected to the vessels at $x = 0$, which is continuously replenished to remove any traces of salt that diffuse out of the vessels, establishes the second constant concentration boundary condition on the diffusion field. In both \mathbb{R}^2 and \mathbb{R}^3 , the pure water reservoir insures that

$$C(0) = 0, \quad (x = 0). \quad (8)$$

2.3 Steady-state solutions to Fick's Law in \mathbb{R}^2 and \mathbb{R}^3

The boundary conditions elucidated in Section 2.2 fix the integration constants α_i and γ_i , which when substituted back into the solution yield the steady-state concentration fields. After a few steps of algebraic manipulation and the substitution of the non-dimensional identities $\beta \equiv w_{max}/w_0$, and $\mathcal{Z} \equiv x/x_{max}$, the solution for the steady-state concentration field in \mathbb{R}^2 can be written as Eq. (9), and the corresponding solution in \mathbb{R}^3 is Eq. (10), namely,

$$\frac{C(x) - C(0)}{C_{max} - C(0)} = \frac{1}{\log(\beta)} \log(1 + (\beta - 1)\mathcal{Z}), \quad (9)$$

and

$$\frac{C(x) - C(0)}{C_{max} - C(0)} = \frac{\beta\mathcal{Z}}{1 + (\beta - 1)\mathcal{Z}}. \quad (10)$$

Equations (9) and (10) provide the desired expressions for arbitrary values of the widths of w_0 and w_{max} . By decreasing w_{max} while increasing w_0 , the shape of the funnel vessel may be altered as follows: a) to one that has a narrow opening at the pure water interface and a broad base where the salt layer is placed; b) to one that has equal values, creating either a rectangular diffusion channel in \mathbb{R}^2 , or a right-circular cylindrical diffusion channel in \mathbb{R}^3 ; or c) to one that has a broad opening at the pure water interface and a narrow base where the salt layer is placed. Steady-state concentration plots calculated from these analytical solutions are displayed in Figure 3 for seven different funnel geometries. As shown in Equations 9 and 10, the fields depend only on the ratios $\mathcal{Z} \equiv x/x_{max}$ and $\beta \equiv w_{max}/w_0$. A concave down concentration field occurs when $w_{max} > w_0$. If $w_{max} = w_0$, then the concentration profile is linear in x . If $w_{max} < w_0$, then the concentration field is concave up.

3 Random Walk Simulations in \mathbb{R}^2

The random walk simulation of the diffusion exchange of salt and water molecules was conducted only in two dimensions for reasons of efficiency and

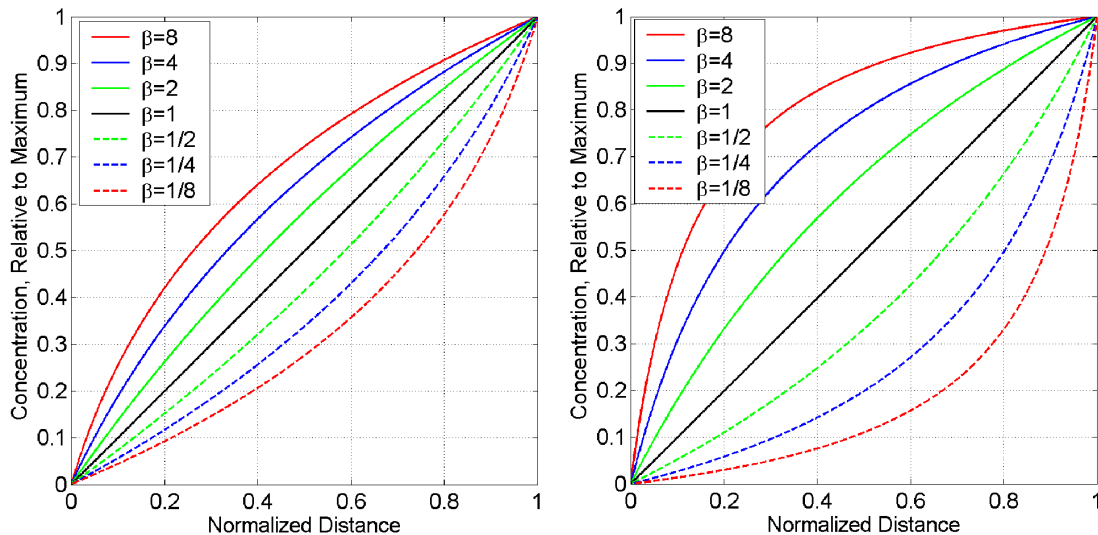


Figure 3: **Left:** Continuum analytical solutions to Fick’s second law in \mathbb{R}^2 from Eq. (9). **Right:** Continuum analytical solutions to Fick’s second law in \mathbb{R}^3 from Eq. (10). The dimensionless parameter β describes the shape of the diffusion channel.

accuracy of the data, and reducing CPU time. The Matlab[©]-based computer code for these simulations was developed at Rensselaer Polytechnic Institute [16, 17].

3.1 Simulation Rules

Our simulation was initiated by choosing the number of random walks to be averaged, the number of steps comprising each walk, the step length, and selecting specific values for w_{max} and w_0 . The results shown in this paper were obtained for the fixed step length, λ —actually the standard deviation of a Gaussian random process—which was fixed at $\lambda = 0.1$. Along with the choice of $\lambda = 0.1$, the number of steps, n , was fixed at 10,000. This choice ensured that particles were able to make multiple trips over the full length of the diffusion path, which was fixed at $\ell_{diff} = 10$. These choices assure satisfaction of the steady-state requirement.

The Matlab[©] code begins by randomly and uniformly distributing water molecules within the rectangle defined by the height of the funnel vessel and its maximum width, $2w_{max}$. Each water molecule is placed randomly, without

taking into account the current positions of any other water molecules. The number of calls sent to the random number generator was set so that any given unit area contains approximately 100 water molecules. Thus, if $2w_{max}$ were the largest dimension of the diffusion channel, then it defined the width of the simulation rectangle. However, if two times $2w_0$ were the largest channel dimension, then this dimension was used to create the simulation rectangle. For the case of a rectangular channel, which is defined as having a height of 10 units and a width of $2w_0 = 2w_{max} = 1$ unit, there are 1000 water molecules present at the beginning of the simulation. Over the course of the simulation the total number of molecules does not change, but their “identity” does, as will be explained below. The identical procedure was used for tapered

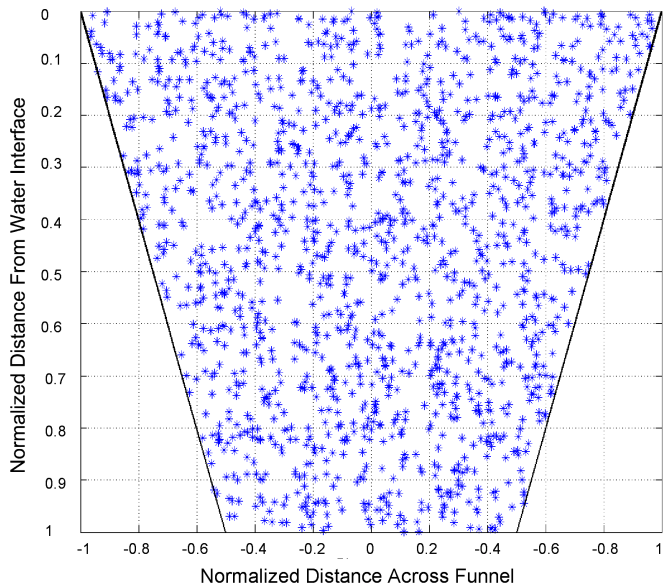


Figure 4: Initial placement of water molecules as random walkers.

diffusion channels when $w_{max} \neq w_0$. Water molecules were placed randomly and uniformly throughout the largest possible rectangle. All of the walkers that lay outside the boundary defined by Eq. (4) were deleted, and only walkers residing within the defined boundaries were tracked as the simulation progressed. For the cases where $w_{max} = 2w_0$ or $w_0 = 2w_{max}$, the resulting rectangle used in the initial placement of the water molecules has a width of 2 units and a height of 10 units. The result of this rule was that 2000 points were placed in the rectangle. After the boundary lines were drawn,

approximately 500 points were eliminated, leaving approximately 1500 points in the diffusion simulation. Figure 4 shows the initial placement of the water molecules when w_0 is twice as large as w_{max} .

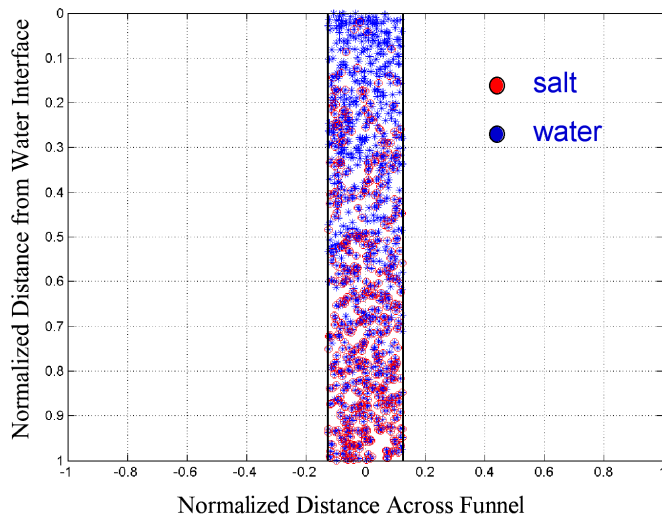


Figure 5: Simulation results for the steady-state distribution of salt and water molecules diffusing through a rectangular vessel, $\beta=1$.

By placing the walkers initially within a rectangle, and then tracking only the walkers residing within the defined boundaries of the diffusion channel, each funnel had approximately the same density of uniformly distributed walkers. Once the simulations started, every walker moved once per cycle, without taking into account the positions of the other walkers. When a walker of either salt or water encountered the horizontal boundary located at w_{max} , the walker was deemed to be salt molecule. By contrast, if a salt molecule diffused all the way to the top of the diffusion channel and encountered the boundary located at w_0 , the salt molecule would be “converted” into a water molecule. In addition to changing the nature of the molecules that encounter the limiting horizontal boundaries, w_0 and w_{max} , these boundaries also act as perfectly reflecting diffusion barriers. Thus, the transformed walkers do not accumulate at either horizontal boundary. The side boundaries also act as reflecting barriers for both water and salt molecules. Both types of walkers underwent elastic collisions with the side walls and were reflect back into the diffusion channel without changing from one molecular type to the other.

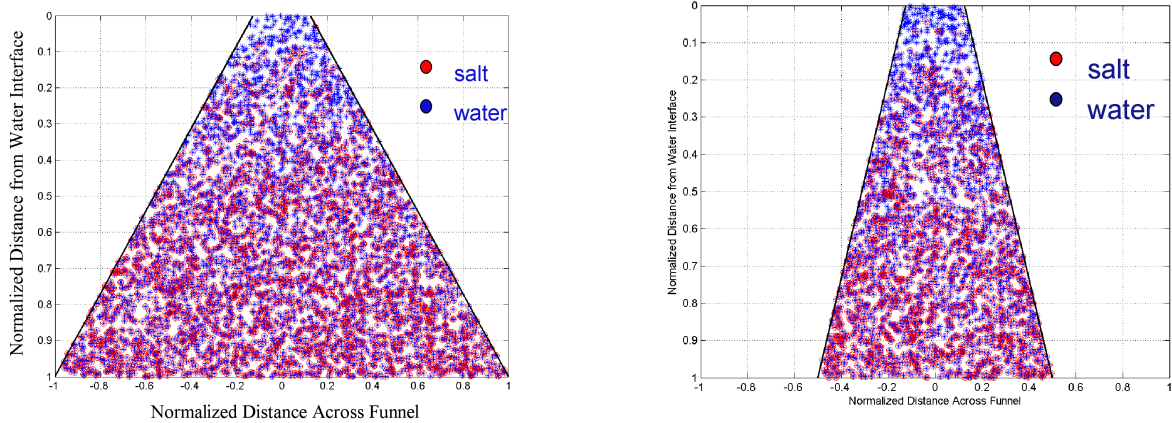


Figure 6: **Left:** Steady-state simulation of diffusion in a tapered channel, $\beta = 8$. **Right:** Steady-state simulation of diffusion in a tapered channel, $\beta = 4$.

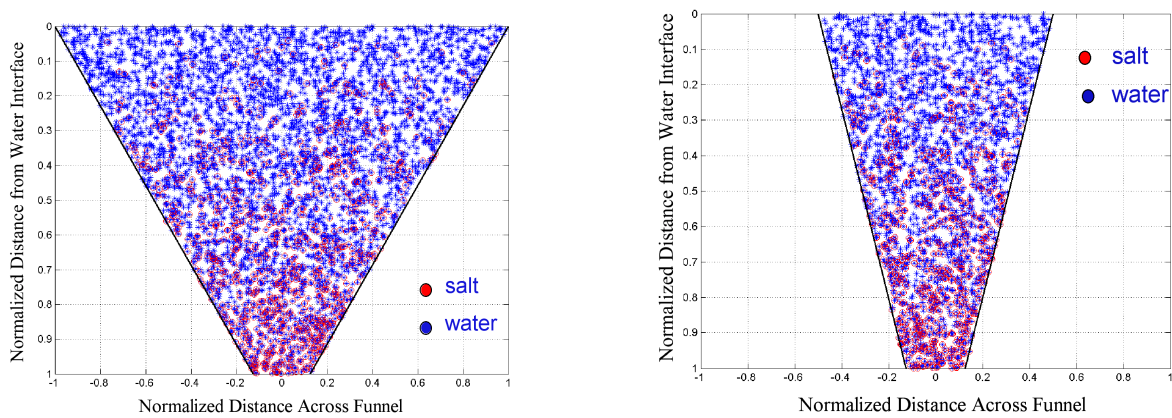


Figure 7: **Left:** Steady-state simulation of diffusion in a tapered channel, $\beta = 1/8$. **Right:** Steady-state simulation of diffusion in a tapered channel, $\beta = 1/4$.

Because the simulation explicitly took into account what happens when one type of walker encounters the opposing boundary, it was unnecessary to control the step length in order to eliminate so-called edge effects. Selection of the step length, λ , became important, however, when determining the number of steps needed in the random walk to yield accurate results, which complied with the required steady-state diffusion conditions. The larger the step length, the fewer the number of steps in the random walk that were required to achieve sufficient walker displacements. Initial testing showed that a step length of $\lambda = 0.1$, combined with $n = 10,000$ steps in the random walk, yielded consistent steady-state results of sufficient accuracy for the present

purposes.

3.2 Simulation Results

Figures 5, 6, and 7 show the results of several simulated cases for different diffusion channel contours. These data plots show the parameter, β , establishing the channel shape, and the steady-state position of all of the molecules in the final walk of the 100 trials used to compute the average concentration. In these plots, the blue points represent water molecules and the red points represent salt molecules. In order to keep track of the concentration gradient

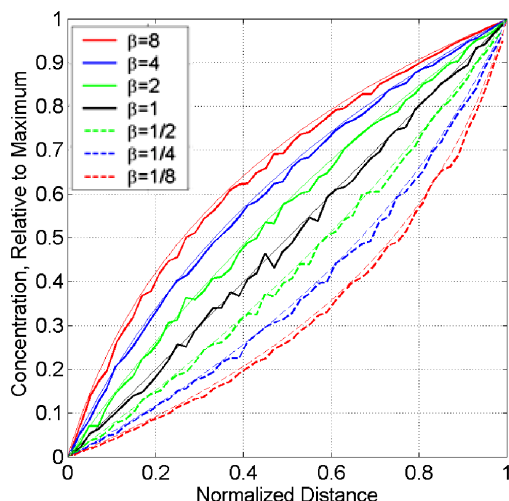


Figure 8: Theoretical predictions and simulation of interdiffusion in two dimensions, correlated for different channel shapes (β ratios). The smooth lines are predictions derived from continuum theory, Eq. (9). The jagged lines represent simulation data based on random walk trials.

accurately as the number of steps in the random walk increased, each funnel-shaped diffusion path was divided into 50 horizontal bins. Thus, the plot of normalized concentration, Figure 8, shows the number of particles in a bin 0.2 wide as a single point. These points are then connected by straight-line segments to give the jagged lines seen in Figure 8. Each of the simulation results shown as bold lines was produced by averaging 100 walks. The simulation curves are compared to the continuum theoretical results for the same β ratio, shown by the corresponding smooth curves. Figure 8 clearly shows

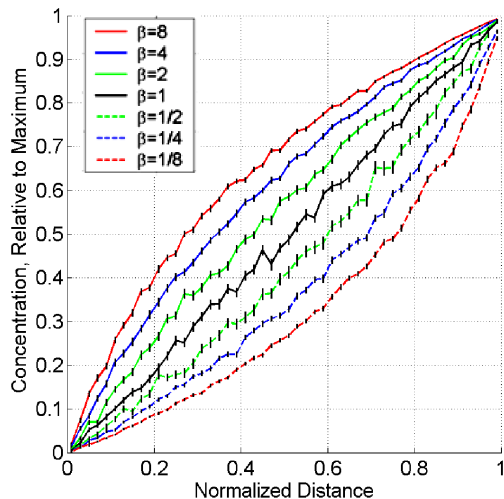


Figure 9: Random walk simulation results with error bars for different β ratios.

the alteration of the concentration field with respect to the vessel's shape. The simulation results agree with the continuum theoretical results for every case investigated. Averaging more than 100 walks for each funnel shape would doubtless improve the agreement between the simulation and theoretical results.

The error bars associated with the average of 10,000 random walks are shown in Figure 9. Both the continuum theoretical predictions and the simulations remain within one standard deviation, considering that the error bars represent a relative error of approximately $\pm 10\%$ for each point. It is especially important to note that steady-state conditions for diffusion must be met before the random walk data yield an acceptable approximation to the analytical predictions based on steady-state continuum theory. For this particular simulation, the steady-state condition was achieved only after the particles had diffused several times from one end of the tapered channel to the other. Even after averaging one hundred 5000 step walks, the random walkers representing salt molecules just reached the position denoted as w_0 . As a result, the steady-state condition had not yet been achieved. It takes approximately $n = 10,000$ steps with a step length $\lambda = 0.1$ to achieve the steady-state condition. Only then does the random-walk simulation of steady-state diffusion provide sufficiently good agreement with the analytical continuum results.

4 Conclusions

Fick's second law was checked numerically by simulating his famous funnel experiments of 1855, where the diffusive flow area can vary. Following the derivation of Fick's second law in two and three dimensions, a random walk simulation in two dimensions was used to verify two-dimensional continuum theoretical results. These results show that with a sufficiently large number of trials, lengthy random walks can in fact be used to simulate with controlled errors the results obtained from Adolf Fick's original salt experiments. Steady-state continuum diffusion solutions compare remarkably well with random walk statistics. To obtain accurate simulation results, steady-state conditions must be achieved in the simulations. This requires that the molecules travel the length of the diffusion channel at least once. The step length, λ , and number of individual steps, n , can be adjusted to ensure that this condition is met. The larger the step length, the fewer is the number of steps needed to achieve steady-state diffusion conditions. As with any random walk simulation, the more trials that are included in reporting the average, the better is the agreement obtained with continuum theory.

References

- [1] M.H. Jacobs, *Diffusion Processes*, Springer, New York, 1967.
- [2] A. Fick, *Pogg. Ann. Phys. Chem.*, **91** (1854) 287-290.
- [3] A. Fick, *Poggendorff's Annalen*, **94**, 3, (1855) 59-86.
- [4] A. Fick, *Philos. Mag.*, **10** (1855) 30-39.
- [5] A. Fick, *Z. für rat. Medicine*, **6** (1855) 288-301.
- [6] A. Fick, *Liebig Ann. Chem.*, **102** (1857) 97-101.
- [7] J. Philibert, "Adolph Fick and Diffusion Equations", *Proceedings of DiSo Conference*, Moscow, Russia, 2005.
- [8] E.L. Cussler, *Diffusion: Mass Transfer in Fluid Systems*, Cambridge University Press, 1984.
- [9] J. Philibert, *Atom Movements: Diffusion and mass transport in solids*, translated by S.J. Rothman, Les Editions de Physique, 1991.

- [10] J. Crank, *The Mathematics of Diffusion*, 2nd ed., Clarendon Press, Oxford, 1994.
- [11] E.B. Watson, “Diffusion in Volatile-Bearing Magmas”, In, *Reviews in Mineralogy*, **30** (1994) 379-401.
- [12] M.E. Glicksman, *Diffusion in Solids: Field Theory, Solid-State Principles, and Applications*, John Wiley and Sons Inc., New York, 2000.
- [13] J.B.J. Fourier, “The Analytical Theory of Heat”, trans. by A. Freeman, University Press, Cambridge, 1878.
- [14] H.S. Carslaw and J.C., Jaeger, *Conduction of Heat in Solids*, Clarendon Press, Oxford, 1959.
- [15] A. Lupulescu and M.E. Glicksman, *Kinetics Lecture Modules*, Spring 2005. Available at URL (http://www.rpi.edu/dept/materials/in_pe.htm).
- [16] T.W. Patzak, “Fick’s Diffusion Experiments Revisited”, unpublished. Available at URL (<http://petroleum.berkeley.edu/papers/patzek/Fick%20Revisited%20V2.pdf>)
- [17] M.E. Glicksman, R. DiDomizio, and A. Lupulescu, “Theory and Simulation of Fick’s Verification of the 2nd Law”, Abstract in the conference “Diffusion Fundamentals”, Leipzig, Germany, 2005.
- [18] R. DiDomizio, “Random Walk Simulation of Fick’s Salt Experiments.” Term project for *Diffusion in Solids*, Rensselaer Polytechnic Institute, 2002. Unpublished.
- [19] M.E. Glicksman, Personal Communication, 2004.